

Title: Collagen Density Modulates the Immunosuppressive Functions of Tumor-Associated Macrophages

Authors: Anne Mette H. Larsen^{1,2}, Dorota E. Kuczek¹, Adrija Kalvisa³, Majken S. Siersbæk³, Marie-Louise Thorseth¹, Marco Carretta¹, Lars Grøntved³, Ole Vang², Daniel H. Madsen^{1,4}

Affiliations:

¹ Center for Cancer Immune Therapy, Department of Hematology, Copenhagen University Hospital Herlev, Herlev, Denmark.

² Institute for Science and Environment, Roskilde University, Denmark.

³ Department of Biochemistry and Molecular Biology, University of Southern Denmark, Odense, Denmark.

⁴ Department of Oncology, Copenhagen University Hospital Herlev, Herlev, Denmark.

Corresponding author: Daniel Hargbøl Madsen

E-mail: daniel.hargboel.madsen@regionh.dk

Key words: Tumor microenvironment; tumor-associated macrophages; extracellular matrix; immune modulation; tumor immunology; mechanosensing; 3D culture

Abstract

Background

Tumor-associated macrophages (TAMs) are known to support tumor growth by suppressing the activity of tumor infiltrating T cells. Consequently, the number of TAMs has been correlated with a poor prognosis of cancer. However, the molecular reason why TAMs acquire an immunosuppressive phenotype is still not completely understood. During solid tumor growth, the extracellular matrix is degraded and substituted with a tumor specific high-density collagen-rich extracellular matrix. The collagen density of the tumor extracellular matrix has been associated with a poor prognosis of several cancers, but the reason for this is still unknown. Here, we have investigated if the pro-tumorigenic effects of collagen density could involve the modulation of TAM functions.

Methods

In this study, the macrophage cell line RAW 264.7 was cultured in 3D collagen matrices of low- and high collagen densities mimicking healthy and tumor tissue, respectively. Using this model, the effects of collagen density on macrophage phenotype and function were investigated by confocal microscopy, flow cytometry, RNA sequencing, qRT-PCR, and ELISA analysis. To investigate the effect of collagen density on the immune modulatory activity of macrophages, co-culture assays with primary T cells to assess T cell chemotaxis and T cell suppression were conducted.

Results

Collagen density did not affect the proliferation, viability or morphology of macrophages. However, whole-transcriptome analysis revealed that the expression of several immune regulatory genes and genes encoding chemokines were differentially regulated between cells grown in low- and high-density collagen. Key findings were confirmed using qRT-PCR analysis and ELISA. Strikingly, the gene regulations had clear functional consequences. Macrophages grown in high-density collagen were less efficient at attracting cytotoxic T cells and at the same time capable of inhibiting T cells proliferation to a greater extent than macrophages grown in low density collagen.

Conclusion

Our study shows that increased collagen density creates a more immunosuppressive phenotype of macrophages. This could be one of the mechanisms linking increased collagen density to poor patient prognosis.

Introduction

Immunotherapy is a new promising way of treating cancer, using the host's own immune response to fight the disease. Various kinds of immunotherapies are available, using different strategies to induce T cells to kill the cancer cells^{1,2}. Checkpoint-inhibitor therapy (anti-CTLA4 and anti-PD-1) and adoptive T cell transfer are two of the most successful types of immunotherapies^{1,2}. They both exploit the ability of endogenous T cells to recognize and kill cancer cells. Unfortunately, not all patients respond to immunotherapy and some patients only display a partial response followed by relapse³. A likely explanation is the existence of an immunosuppressive tumor microenvironment (TME), which inhibits the activity of tumor-infiltrating T cells and thereby reduces the efficiency of the treatment^{4,5}. The mechanisms underlying the generation of an immunosuppressive TME are still only partially understood.

During solid tumor growth, the surrounding extracellular matrix (ECM) is degraded and substituted with a different tumor specific ECM. This often contains high amounts of collagen type I, which is the main ECM component, is more linearized and of increased stiffness^{6,7}. The density and structure of this tumor specific ECM have been linked to a poor prognosis of several cancers such as breast cancer, pancreatic cancer, and oral squamous cell carcinomas⁷⁻¹⁰, but the reason for this correlation is still not clear. Studies have shown that the density and stiffness of the ECM can affect various cell types, including, mesenchymal stem cells¹¹, fibroblasts^{12,13}, and cancer cells^{7,14,15}. However, very little is known about the effect of the ECM on tumor-associated macrophages (TAMs).

TAMs often acquire an anti-inflammatory phenotype and are known to support tumor growth through various mechanisms such as suppression of tumor-infiltrating T cells¹⁶⁻¹⁸. This immunosuppressive activity of TAMs is considered a major limitation for the efficiency of immunotherapy, and consequently, the number of TAMs has been correlated with a poor prognosis in many types of cancer¹⁹⁻²¹. Therapeutic approaches have already been tested in mice, aiming at re-programming TAMs toward a more pro-inflammatory phenotype^{22,23}. These have shown promising results in various cancers, but the molecular reason why TAMs gain an immunosuppressive phenotype in the TME is still not completely understood.

Macrophage are very plastic cells, which can change their phenotype and function depending on external cues. These cues include the mechanical stiffness of the substrates to which the macrophages adhere²⁴⁻²⁶. Furthermore, the interactions with collagen type I has been shown to induce a more anti-

inflammatory phenotype of alveolar macrophages²⁷. The possibility that collagen density within tumors can affect the phenotype of TAMs has not been studied, but recently it was demonstrated that implantation of a collagen gel into an injured muscle of a mouse, stimulated T cells to become less cytotoxic and macrophages to become more immunosuppressive²⁸. This suggests, that collagen could also influence the immunosuppressive properties of macrophages in the TME.

In this study we used 3D culture assays to investigate if collagen density could drive the generation of immunosuppressive macrophages in the TME.

Materials and Methods:

RAW 264.7 preparation and culture in 3D collagen matrices.

The murine macrophage cell line RAW 264.7 was cultured in RPMI supplemented with 10% FBS and 1% P/S for no more than 20 passages and split one day prior to 3D culture in collagen matrices. 3D type I collagen matrices were prepared based on the protocol by Artym and Matsumoto²⁹. Briefly, collagen matrices were generated by mixing rat tail collagen type I (Corning), 0.02N acetic acid, 10x DMEM with phenol red (Sigma Aldrich) and 10x reconstitution buffer (0.2M Hepes (Gibco) and 0.262M NaHCO₃). To neutralize the pH, 2N NaOH was added to the reconstitution buffer prior to use. First, 350 µl collagen solution of either low- (1 mg/ml) or high (4 mg/ml) collagen density was prepared and added to wells of a non-tissue culture treated 24-well plates (Corning). The collagen solution was allowed to polymerize for at least 1h at 37°C, 5% CO₂. Next, 350 µl collagen solution containing 60,000 RAW 264.7 macrophages was added onto the first collagen gel of matching concentration. The gel was allowed to polymerize for 2-3h after which 600 µl prewarmed RPMI supplemented with 10% FBS and 1% P/S was added on top of the collagen gel. To remove salt and potentially unpolymerized collagen present, the media was changed twice on all samples after 24h of culture. For conventional 2D culture, 60,000 cells per sample were seeded in tissue-culture treated 24-well- or 6-well plates.

Confocal microscopy

3D collagen matrices of 1 mg/ml or 4 mg/ml collagen were made as previously described but with additionally 20% acid-extracted rat tail tendon type I collagen labelled with Alexa Fluor 647 incorporated. The Alexa Fluor labelling was done as previously described². A total volume of 200 µl collagen solution containing 60,000 RAW 264.7 macrophages was added per well of a glass bottom 24-well, No. 0 Coverslip, 13 mm Glass Diameter (MatTek Corporation) and allowed to polymerize for 45 min at 37°C, 5% CO₂. Thereafter, 500 µl of RPMI supplemented with 10% FBS and 1% P/S was added on top of the matrices. Prior to microscopy, samples were stained as described by Artym and Matsumoto¹. Briefly, samples were fixed with 4% formaldehyde, 5% Sucrose for 1h and permeabilized with 0.5% Triton-X for 10 min. Next, F-actin and nuclei were stained with 1:40 diluted Alexa Fluor® 488 Phalloidine (Thermo Fisher Scientific) and 1:1000 diluted DAPI (Sigma Aldrich) for 1h and 20 min., respectively. Confocal imaging was performed using an IX83 Olympus confocal microscope equipped with a scanning head (FluoView 1200; Olympus). All images were acquired using an Olympus UPlanSApo 60x/1.35na Oil Objective.

Proliferation and viability of RAW 264.7 macrophages

The proliferation of RAW 264.7 macrophages was determined using an APC BrdU Flow Kit (BD Biosciences) according to the manufacturer's protocol. Briefly, 60,000 RAW 264.7 macrophages were 3D cultured in collagen matrices of either 1 mg/ml or 4 mg/ml collagen density or 2D cultured on tissue culture treated 6-well plates for three days. To label the cells, all samples were pulsed with a final concentration of 10 μ M BrdU for 1h. As a negative control, four samples were incubated with 3 μ g/ml Aphidicolin (Sigma Aldrich) together with the BrdU. Following labelling, culture media was aspirated from both 2D and 3D samples, and all samples were treated with 500 μ l 3 mg/ml collagenase type I (Worthington) for 45-60 min. at 37°C, 5% CO₂. Cell solutions were then collected and washed once with DPBS (Lonza) before staining with Zombie Aqua Fixable Viability Dye (BioLegend). Next, cells were fixated, permeabilized and stained with APC anti-BrdU antibody according to the manufacturer's protocol (BD Biosciences). Cells were resuspended in FACS Buffer (DPBS with 5 mM EDTA and 0.5% BSA) and run on a BD™ LSR II Flow Cytometer. Data were analyzed using FACS Diva® 8.0.2 software.

RNA sequencing

RAW 264.7 macrophages were isolated from 3D collagen matrices of 1 mg/ml or 4 mg/ml collagen and from 2D tissue-culture treated 6-well plates. RNA was extracted using the RNeasy Mini Kit (Qiagen). The quantity and purity of isolated RNA were assessed using an Agilent 2100 BioAnalyzer (Agilent Genomics). Total RNA (1000 ng) was prepared for sequencing using polydT-mediated cDNA synthesis in accordance with the manufacturer's (Illumina) instructions. Libraries were made with a NEBNext RNA Library Preparation Kit for Illumina. Library quality was assessed using Fragment Analyzer (AATI), followed by library quantification (Illumina Library Quantification Kit). Sequencing was done on a HiSeq1500 platform (Illumina) with a read length of 50 bp. Sequenced reads were aligned to *mus musculus mm9* using STAR³⁰. Uniquely aligned reads were quantified at exons of annotated genes and normalized to sequence depth and gene length using HOMER³¹. The number of reads per kilobase per million mapped (RPKM) for all RefSeq annotated genes can be found in Table S1. The analysis of differential expression was performed using DESeq2 package in R. Principal component analysis was performed using R (prcomp package). GOSeq analysis were performed with R, using only data with FDR < 0.05 and Log2FoldChange +/- 0.584962501. Heatmaps were generated from z-score normalized RPKM values using R (pheatmap package) on selected sets of genes. MA plots and Volcano plots were generated from RPKM values using R.

RNA extraction, cDNA synthesis and quantitative real-time-PCR

RNA was isolated from RAW 264.7 macrophages cultured in 3D collagen matrices of 1 mg/ml or 4 mg/ml collagen and from 2D tissue-culture treated 6-well plates as previously described. The quantity and purity of isolated RNA were assessed using an Agilent 2100 BioAnalyzer (Agilent Genomics). cDNA was generated using iScript™ cDNA Synthesis Kit (Bio Rad). As a control, a noRT sample were included during the cDNA synthesis, containing all components but the reverse transcriptase. The qRT-PCR reaction was made using the Brilliant III Ultra-Fast SYBR® Green QPCR Master Mix (Agilent Technologies). Equal amounts of cDNA were added to all samples. As a control, a No Template Control sample containing only the SYBR green master mix were added to the analysis. All samples were run on an AriaMX Real Time PCR System (G8830A). All measurements were based on quadruplicates of each cell culture condition and normalized to the internal reference gene, actin- β . The comparative cycle threshold ($\Delta\Delta CT$) method was used to calculate the relative fold changes. Primers were designed using the Primer-BLAST tool (NCBI, NIH). Only primers spanning exon-exon junction, and with a maximum product length of 250 bp was used. Prior to use, the primer efficiency for all primer sets were measured and found to be between 86% and 111%. Primer sequences are listed in Table S2.

CCL3 and PGE₂ ELISA

ELISAs were performed using Mouse MIP-1 alpha (CCL3) ELISA Ready-SET-Go ELISA kit (eBioscience™) and Prostaglandin E2 ELISA Kit (Abcam) according to the manufacturer's instructions. Analysis was done on conditioned media from RAW 264.7 macrophages cultured in 3D collagen matrices of 1 mg/ml or 4 mg/ml collagen. To evaluate the amount of collagen-bound protein, 3D collagen samples were treated with collagenase type II as previously described. All samples were centrifuged for 5 min. 300xG and stored at -20°C prior to use. All measurements were based on quadruplicates of each cell culture condition.

T cell isolation

T cells were isolated from BALB/c mice spleens using CD3 ϵ MicroBead Kit, mouse (Miltenyi Biotec). Briefly, single cell suspensions were generated by forcing freshly isolated BALB/c mice spleens through 70 μ m cell strainers using the piston of a syringe. Red blood cells were lysed using Red Blood Cell Lysis Buffer (Qiagen) for 1 min. at room temperature. The T cell isolation was done according to the manufacturer's protocol, however prolonging the incubation with CD3 ϵ -Biotin to 20 min. and anti-Biotin to 25 min. Following the isolation, the CD3 negative and positive fraction were stained with CD3-FITC (BioLegend) and Zombie Aqua Fixable Viability Dye (BioLegend) and run

on a BD™ LSR II Flow Cytometer to evaluate the purity. A purity >80% living CD3⁺ cells was considered satisfactory for use in further experiments. A total of 4x10⁶ isolated T cells per well were rested O.N. in RPMI supplemented with 10% FBS and 1% P/S, 50 μM 2-mercaptoethanol, 0.1 mM non-essential amino acids, 1mM Sodium Pyruvate, and 5 μg/ml Concanavalin A (Sigma Aldrich) (From now on referred to as T cell media) in tissue-culture treated 24-well plates.

T cell proliferation assay

For co-culture assays, splenocytes were isolated from spleens of BALB/c mice as previously described. RAW 264.7 macrophages were cultured in 3D collagen matrices of 1 mg/ml or 4 mg/ml collagen for one day prior to co-culture. T cell media was added on top of the 3D collagen and a total of 400,000 freshly isolated splenocytes in T cell media were added to 6.5 mm transwell inserts with 0.4 μm pore polyester membrane (Corning) above the 3D collagen matrices corresponding to a 3:1 ratio of T cells to RAW 264.7 macrophages. As a control, splenocytes were cultured alone above T cell media or collagen matrices of 1 mg/ml or 4 mg/ml collagen without any embedded RAW 264.7 macrophages. Cells were co-cultured for three days. T cell proliferation was determined using an APC BrdU Flow Kit (BD Biosciences) according to the manufacturer's protocol. Briefly, to label the cells, all samples were pulsed with a final concentration of 10 μM BrdU for 1h. As a negative control, four samples were incubated with 3 μg/ml Aphidicolin (Sigma Aldrich) together with the BrdU. Splenocytes were then collected by resuspension and washed ones with DPBS (Lonza) before staining with Zombie Aqua Fixable Viability Dye (BioLegend) and CD3-FITC (BioLegend). Next, cells were fixed, permeabilized and stained with APC anti-BrdU antibody according to the manufacturer's protocol (BD Bioscience). Cells were resuspended in FACS Buffer (DPES+5 mM EDTA+0.5% BSA) and run on a BD™ LSR II Flow Cytometer. Data were analyzed using FACS Diva® 8.0.2 software. Measurements were based on triplicated or quadruplicates of each cell culture condition.

Migration assay

To investigate the ability of macrophages to attract T cells, migration of primary murine T cells towards conditioned media from RAW 264.7 macrophages was measured. Migration assays were performed using O.N. rested primary murine T cell isolated as previously described. Conditioned media was harvested from RAW 264.7 macrophages grown for three days in 3D collagen matrices of 1 mg/ml or 4 mg/ml collagen. A total of 300,000 O.N. rested T cells in a volume of 200 μl were added to 6.5 mm transwell inserts with 5.0 μm pore polycarbonate membranes (Corning). The T cells were

placed above 500 μ l conditioned media in 24-well plates. Prior to use, conditioned media were centrifuged at 300xG for 5 min. and added Concanavalin A (Sigma Aldrich) to a final concentration of 3 μ g/ml. As a control for maximum migration 300,000 T cells were added directly to the wells of a 24-well plate. The T cells were allowed to migrate towards the conditioned media for 26-28h at 37°C, 5% CO₂. Subsequently, all migrated cells were collected from the lower wells and stained with CD3-FITC, CD4-BV421, CD8-APC, CD25-PerCP-Cy5.5 and Zombie Aqua Fixable Viability Dye (All BioLegend). The lower wells were additionally washed ones with FACS buffer to ensure the collection of all cells. To determine the number of migrated cells, all samples were resuspended in 200 μ l FACS Buffer (DPES+5 mM EDTA+0.5% BSA) and run on a BD™ LSR II Flow Cytometer for 2 min. on flow rate “high”. Specific migration was determined by normalizing the data to the maximum control.

Statistical analysis

All experiments were performed at least three times with at least three replicates per condition. All results are presented as the mean +/- standard deviation unless otherwise specified. For two-group comparisons of the means from independent experiments, paired two-tailed Student's t-tests were performed unless otherwise specified. For multi-group comparisons, one-way analysis of variance (ANOVA) was used followed by un-paired two-tailed Student's t-tests unless otherwise specified. All statistical analyses, except RNASeq data, were performed using GraphPad Prism. A p-value <0.05 was considered statistically significant. Statistical analysis of RNASeq data were done using R.

Results

Collagen density does not affect the viability and proliferation of macrophages

Macrophages are known to be very plastic cells, which can change phenotype and function depending on external stimuli. To investigate if 3D culture of macrophages in collagen matrices of different densities affects viability and proliferation, the murine macrophage cell line RAW 264.7 was cultured in 3D collagen matrices of low (1 mg/ml) or high (4 mg/ml) collagen densities or on regular tissue-culture treated plastic (2D culture). The RAW 264.7 cell line were chosen because it is a stable and appropriate model for macrophages³². The selected collagen concentration of 1 mg/ml is representative of healthy normal tissue such as lung or mammary gland, whereas 4 mg/ml collagen mimics the ECM found in solid tumors^{14,33}. To ensure 3D cultured cells were not in contact with any plastic, a lower layer of collagen was generated before adding a second layer of collagen containing RAW 264.7 macrophages. Using confocal microscopy, we confirmed that the RAW 264.7 macrophages were completely surrounded by collagen fibers and located in different planar levels of the matrix (Figure 1A). Additionally, it was clearly seen that the structure and density of collagen was different when comparing low and high collagen density matrices (Figure 1B-C). The different collagen densities did, however, not affect the morphology of the RAW 264.7 macrophages.

To evaluate if 3D culture affected the viability of the macrophages, RAW 264.7 macrophages were cultured in collagen matrices of low or high density and isolated by a brief collagenase treatment. The cells were stained with a live/dead marker and analyzed by flow cytometry (Figure 1D). 3D culture of RAW 264.7 macrophages in collagen matrices did not affect the viability of the cells compared to cells subjected to conventional 2D culture on a plastic surface (Figure 1D). Additionally, no difference in viability was observed between cells cultured in low density collagen compared to cells cultured in high density collagen (Figure 1D). Next, the proliferation of the cells was evaluated using a BrdU-based flow cytometer assay (Figure 1E). Neither culture of the cells in 3D compared to 2D nor culture of the cells in collagen of different densities affected the proliferation of the RAW 264.7 macrophages (Figure 1E).

3D culture affects the transcriptional profile of macrophages.

Although 3D culture in different collagen densities did not affect the morphology, viability, or proliferation of RAW 264.7 macrophages, we speculated that the transcriptional profile of the cells could still be affected. To investigate this possibility, RNA was extracted from RAW 264.7 macrophages cultured in collagen matrices of low or high densities or on 2D tissue-culture treated plastic and subjected to RNA sequencing. A Principal Component Analysis of the resulting data, strikingly showed

that the transcriptional profile of macrophages cultured in 3D (low and high density) separate from the 2D cultured macrophages and also that macrophages cultured in high-density collagen cluster separately from macrophages cultured in low-density collagen (Figure 2A). Additional analysis of the difference between 3D and 2D culture revealed that 1270 and 1490 genes (FDR=0.01, Fold change > 0.584962501) were significantly regulated when comparing cells cultured on 2D tissue culture treated plates with cells 3D cultured in low density collagen (Figure 2B, Figure S1 and table S3) and high density collagen (Figure S1-S2 and table S4), respectively. The full gene expression dataset is in Table S1. To investigate which biological processes the regulated genes were involved in, gene ontology analysis was performed. Within genes upregulated in cells 3D cultured in low density collagen compared to cells cultured on 2D tissue-culture treated plastic, *cell adhesion* and *biological adhesion* were most significantly enriched (Figure 2C). Downregulated genes were especially involved in the biological processes *single organism signaling* and *signaling* (Figure 2D).

To investigate which transcription factor motifs that could be responsible for the gene expression changes observed in 3D cultured RAW 264.7 macrophages we used the computational method IS-MARA (Integrated Motif Activity Response Analysis, <https://ismara.unibas.ch/mara/>), which models transcription factor activity using RNA sequencing data³⁴. When comparing cells 3D cultured in low density collagen to regularly 2D cultured cells, it was found that among the identified upregulated transcription factor motifs, TEAD and SMAD were listed (Figure S3A-B). These are known to be regulated by the mechanosensing YAP/TAZ pathway, which is activated by external mechanical cues such as extracellular matrix stiffness³⁵. Consistently, many genes known to be affected by YAP/TAZ signaling were regulated when comparing cells grown in low density collagen to 2D cultured cells (Figure S3C). This suggests that YAP/TAZ signaling could be centrally engaged in the 3D culture-induced gene regulations.

Next, the gene expression levels of a panel of immune modulatory genes and a panel of genes encoding chemokines were visualized (Figure 2E-F). Although several genes in both of the panels were significantly regulated, the heatmaps did not clearly show how the immune modulatory functions of the cells were affected by 3D culturing compared to 2D culturing (Figure 2E-F).

Collagen density regulates genes associated with immune regulation and chemoattraction.

Next, the transcriptional differences between RAW 264.7 macrophages cultured in low and high density collagen matrices were investigated. 385 genes were regulated (FDR=0.01, fold change > 0.584962501) when comparing cells cultured in high density collagen to cells cultured in low density

collagen (Figure 3A, S2 and table 1). Of these, 233 genes were upregulated, and in a gene ontology analysis it was found that they were involved in the biological processes *defense response*, *inflammatory response*, and *immune response* (Figure 3B). Likewise, a gene ontology analysis showed that the 152 downregulated genes were involved in *negative regulation of proteolysis* and *cell surface receptor signaling pathway* (Figure 3C).

To investigate if immune modulatory activities could be affected by collagen density, we examined the gene expression levels of a panel of immune regulatory genes (Figure 3D). Many genes were found to be significantly regulated when comparing cells cultured in high density collagen to cells cultured in low density collagen (Figure 3D), suggesting that collagen density could affect the immune regulatory properties of macrophages. Additionally, the gene expression levels of a panel of chemokines were visualized (Figure 3E). Interestingly, the chemokine profile of RAW 264.7 macrophages cultured in high density collagen was clearly altered. The observed changes suggested a reduced recruitment of cytotoxic CD8⁺ T cells (Downregulation of *Ccl3*, *Ccl4*, *Ccl5*, *Cxcl10* and *Cxcl16*) and an increased recruitment of T regulatory cells (Tregs), MDSCs, macrophages and monocytes (Upregulation of *Ccl2*, *Ccl6*, *Ccl7*, *Ccl17* and *Cxcl14*)³⁶⁻³⁸. Selected gene regulations identified by RNA sequencing were confirmed by qRT-PCR analysis using RNA extracted from three independent experiments (Figure 2F).

To investigate if the gene regulations also resulted in altered protein levels, conditioned media from RAW 264.7 macrophages cultured in low or high density collagen was examined using ELISA (Figure 4). In line with the gene expression analysis, it was found that RAW 264.7 macrophages cultured in high density collagen tend to secrete less CCL3 than macrophages cultured in low density collagen (Figure 4A), although not significantly less. CCL3 is an important chemokine involved in recruitment of cytotoxic CD8⁺ T cells to the tumor microenvironment³⁶. This suggests that macrophages surrounded by a high density collagen matrix could be less efficient at attracting cytotoxic CD8⁺ T cells.

By RNA sequencing, it was found that *Ptgs1* and *Ptgs2* were upregulated in high density collagen compared to cells cultured in low density collagen matrices (Figure 3D). *Ptgs1* and *Ptgs2* encode the two enzymes, COX-1 and -2, which are critical for the synthesis of the prostanoid lipid, Prostaglandin E2 (PGE₂)³⁹. Using ELISA, it was demonstrated that the upregulation of *Ptgs1* and -2 also led to an increased level of PGE₂ in the conditioned media (Figure 4B). Interestingly, a large fraction of the PGE₂ was not released to the conditioned media but was instead bound to the collagen matrix (Figure 4C). Consequently, collagenase treated collagen matrices contained high levels of PGE₂ but again

more PGE₂ was measured when cells were cultured in high density collagen (Figure 4B-C). No CCL3 was found in collagenase treated collagen matrices (data not shown).

Collagen density regulates T cell proliferation through its effects on macrophages.

To investigate if collagen density-induced transcriptional changes had any functional effects on macrophages, we co-cultured primary isolated murine splenocytes with RAW 264.7 macrophages grown in collagen matrices of low or high density (Figure 5A). The splenocytes and RAW 264.7 macrophages were separated by transwell inserts allowing for cell-cell communication through secreted factors. After three days of co-culture, the proliferation of T cells was evaluated using a BrdU-based flow cytometry assay. Initially, it was found that co-culture with RAW 264.7 macrophages embedded in low density collagen inhibited the proliferation of T cells compared to T cells cultured alone (Figure 5B). However, strikingly, RAW 264.7 macrophages grown in high-density collagen were capable of inhibiting T cell proliferation to an even higher degree (Figure 5B). This result indicate that macrophages cultured in high density collagen matrices are acquiring a more immunosuppressive phenotype than macrophages situated in low density collagen matrices. Culture of T cells above collagen matrices of low or high density without any RAW 264.7 macrophages embedded had no effect on T cell proliferation (Figure 5B).

Collagen density alters the chemotactic activity of macrophages.

The chemokine profile of RAW 264.7 macrophages cultured in high density collagen indicated that these would be less efficient at attracting cytotoxic CD8⁺ T cells and more efficient at attracting Tregs (Figure 3E). To investigate this possibility, T cell migration towards the chemokines secreted by RAW 264.7 macrophages was examined. T cells were allowed to migrate towards conditioned media from RAW 264.7 macrophages, which had been cultured in low- or high density collagen (Figure 6A). Strikingly, T cells migrated significantly less towards conditioned media from RAW 264.7 macrophages grown in high density collagen compared to conditioned media from RAW 264.7 macrophages grown in low density collagen (Figure 6B). When investigating the migration of T cell subsets, it was found that especially CD8⁺ T cells migrated less towards the conditioned media from the RAW 264.7 macrophages cultured in high density collagen (Figure 6C). Interestingly, there was a trend that Tregs (CD4⁺/CD25⁺) migrated more towards the conditioned media from RAW 264.7 macrophages grown in high density collagen (Figure 6E). There was no significant difference in the migration of CD4⁺ T cells (Figure 6D). Co-culture of T cells with conditioned media from RAW 264.7 macrophages showed that the RAW 264.7 macrophages did not change the phenotype of the T cells (Figure S4), and thus these differences in migration could only be caused by changes in the chemo attractive

activities of the RAW 264.7 macrophages. The observed effects on T cell migration were confirmed in four independent experiments (Figure S5A-D). The data suggest that macrophages surrounded by a high density collagen matrix become less efficient at recruiting cytotoxic CD8⁺ T cells.

Discussion

Collagen density strongly correlates with poor prognosis in many types of cancer. In this study, we investigated if the correlation could be due to collagen density-induced modulation of TAMs and consequently the generation of an immunosuppressive TME. Using 3D culture of the macrophage cell line RAW 264.7 in collagen type I matrices we examined the response of RAW 264.7 macrophages to the surrounding density of collagen and compared the phenotypes to that of RAW 264.7 macrophages culture on regular tissue culture treated plastic.

The viability and proliferation of RAW 264.7 macrophages were not affected by 3D culture or by changes in the collagen densities but when comparing the gene expression profile of cells cultured in 3D and in 2D, dramatic changes were nevertheless observed. The strong response is consistent with the known plasticity of macrophages and their ability to react to external stimuli. Looking more carefully at the transcriptional changes it was, however, unclear if 3D culture made the macrophages acquire a more immunosuppressive phenotype. A computational analysis of potential transcription factor motifs involved in the 3D culture-induced gene regulations suggested that YAP/TAZ signaling could be centrally engaged.

The comparison of RAW 264.7 macrophages cultured in high density collagen compared to low density collagen revealed that a smaller number of genes were regulated by the surrounding collagen density. Strikingly, however, many genes involved in immune modulation or encoding chemokines were among the regulated genes. To investigate how these transcriptional changes affected the functions of the macrophages, co-culture assay with primary murine T cells were conducted. These experiments demonstrated that RAW 264.7 macrophages cultured in a high density collagen matrix acquire a T cell-suppressive phenotype and become less efficient at attracting cytotoxic CD8⁺ T cells. This identified ability of the collagen density to change the immune regulatory activity of macrophages could be an important molecular mechanism underlying the generation of an immunosuppressive tumor microenvironment. Recently, we showed that a high collagen density can also directly downregulate the cytotoxic activity of T cells and instead make them more regulatory⁴⁰. Together with the findings of this study, these observations suggest that the collagen density within tumors could be centrally engaged in generating an immunosuppressive tumor microenvironment, and indicate that the prognostic value of collagen density could be related to its immune regulatory activity.

Stromal collagen has been suggested by others to prevent the migration of cytotoxic T cells into the tumor islets^{41,42}. Based on our observed changes of the chemokine profile of macrophages, we speculate that a high collagen density could also limit T cell influx by reducing the macrophage-mediated chemoattraction of cytotoxic T cells.

In conclusion, we have identified collagen density as an important driver of macrophage polarization toward a more immunosuppressive phenotype. This immunosuppressive mechanism could be critical for the ability of cancers to evade immune destruction and could constitute a limiting factor for the efficacy of immunotherapy.

Acknowledgments: This study was supported by the Danish Cancer Society (D.H.M.), Knæk Cancer (D.H.M.), Novo Nordisk Foundation (D.H.M.), Dagmar Marshalls Foundation (D.E.K., D.H.M., A.M.H.L.), Dansk Kræftforskningsfond (D.E.K.), Einar Willumsen Foundation (D.E.K.), Jens og Maren Thestrups legat til kræftforskning (A.M.H.L.), Agnes og Poul Friis' Fond (A.M.H.L.), and Herlevs Forskningsfond (A.M.H.L.). We thank Dr. Janine T. Erler for providing BALB/c mice.

Author contributions: Conceptualization, D.H.M. and A.M.H.L.; Methodology, D.H.M., A.M.H.L., D.E.K., L.G., and O.V.; Investigation, D.H.M., A.M.H.L., D.E.K., A.K., M.S.S., M.L.T., M.C., L.G.; Writing – Original Draft, D.H.M. and A.M.H.L.; Writing – Review & Editing, D.H.M., A.M.H.L., D.E.K., A.K., M.S.S., M.L.T., M.C., L.G., and O.V.

References

1. Rosenberg, S. A. & Restifo, N. P. Adoptive cell transfer as personalized immunotherapy for human cancer. *Science (80-.)*. **348**, 62–68 (2015).
2. Sharma, P. & Allison, J. P. The future of immune checkpoint therapy. *Science* **348**, 56–61 (2015).
3. Andersen, R. *et al.* Long-lasting complete responses in patients with metastatic melanoma after adoptive cell therapy with tumor-infiltrating lymphocytes and an attenuated IL-2 regimen. *Clin. Cancer Res.* (2016). doi:10.1158/1078-0432.CCR-15-1879
4. Becker, J. C., Andersen, M. H., Schrama, D. & Thor Straten, P. Immune-suppressive properties of the tumor microenvironment. *Cancer Immunol. Immunother.* **62**, 1137–1148 (2013).
5. Munn, D. H. & Bronte, V. Immune suppressive mechanisms in the tumor microenvironment. *Curr. Opin. Immunol.* **39**, 1–6 (2016).
6. Fang, M., Yuan, J., Peng, C. & Li, Y. Collagen as a double-edged sword in tumor progression. *Tumour Biol.* **35**, 2871–82 (2014).
7. Levental, K. R. *et al.* Matrix Crosslinking Forces Tumor Progression by Enhancing Integrin Signaling. *Cell* **139**, 891–906 (2009).
8. Conklin, M. W. *et al.* Aligned collagen is a prognostic signature for survival in human breast carcinoma. *Am. J. Pathol.* **178**, 1221–1232 (2011).
9. Drifka, C. R. *et al.* Highly aligned stromal collagen is a negative prognostic factor following pancreatic ductal adenocarcinoma resection. *Oncotarget* **7**, In preparation (2016).
10. Li, H.-X. *et al.* Expression of $\alpha\beta 6$ integrin and collagen fibre in oral squamous cell carcinoma: association with clinical outcomes and prognostic implications. *J. Oral Pathol. Med.* **42**, 547–56 (2013).
11. Engler, A. J., Sen, S., Sweeney, H. L. & Discher, D. E. Matrix Elasticity Directs Stem Cell Lineage Specification. *Cell* **126**, 677–689 (2006).
12. Huang, X. *et al.* Matrix stiffness-induced myofibroblast differentiation is mediated by intrinsic mechanotransduction. *Am. J. Respir. Cell Mol. Biol.* **47**, 340–348 (2012).
13. Puig, M. *et al.* Matrix Stiffening and β_1 Integrin Drive Subtype-Specific Fibroblast Accumulation in Lung Cancer. *Mol. Cancer Res.* **13**, 161–173 (2015).
14. Paszek, M. J. *et al.* Tensional homeostasis and the malignant phenotype. *Cancer Cell* **8**, 241–254 (2005).
15. Provenzano, P. P. *et al.* Collagen density promotes mammary tumor initiation and progression. *BMC Med.* **6**, 11 (2008).
16. Lewis, C. E. *et al.* The Multifaceted Role of Perivascular Macrophages in Tumors. *Cancer*

- Cell* **30**, 18–25 (2016).
17. Doedens, A. L. *et al.* Macrophage expression of hypoxia-inducible factor-1 alpha suppresses T-cell function and promotes tumor progression. *Cancer Res.* **70**, 7465–75 (2010).
 18. Noy, R. & Pollard, J. W. Tumor-Associated Macrophages: From Mechanisms to Therapy. *Immunity* **41**, 49–61 (2014).
 19. Kubota, K. *et al.* CD163+CD204+ tumor-associated macrophages contribute to T cell regulation via interleukin-10 and PD-L1 production in oral squamous cell carcinoma. *Sci. Rep.* **7**, 1755 (2017).
 20. Zhang, M. *et al.* A high M1/M2 ratio of tumor-associated macrophages is associated with extended survival in ovarian cancer patients. *J. Ovarian Res.* **7**, 19 (2014).
 21. Biswas, S. K., Allavena, P. & Mantovani, A. Tumor-associated macrophages: functional diversity, clinical significance, and open questions. *Semin. Immunopathol.* **35**, 585–600 (2013).
 22. Georgoudaki, A. M. *et al.* Reprogramming Tumor-Associated Macrophages by Antibody Targeting Inhibits Cancer Progression and Metastasis. *Cell Rep.* **15**, 2000–2011 (2016).
 23. Pyonteck, S. M. *et al.* CSF-1R inhibition alters macrophage polarization and blocks glioma progression. *Nat. Med.* **19**, 1264–72 (2013).
 24. Scheraga, R. G. *et al.* TRPV4 Mechanosensitive Ion Channel Regulates Lipopolysaccharide-Stimulated Macrophage Phagocytosis. *J. Immunol.* **196**, 428–436 (2016).
 25. Blakney, A. K., Swartzlander, M. D. & Bryant, S. J. The effects of substrate stiffness on the in vitro activation of macrophages and in vivo host response to poly(ethylene glycol)-based hydrogels. *J. Biomed. Mater. Res. A* **100**, 1375–86 (2012).
 26. McWhorter, F. Y., Davis, C. T. & Liu, W. F. Physical and mechanical regulation of macrophage phenotype and function. *Cell. Mol. Life Sci.* **72**, 1303–16 (2015).
 27. Stahl, M. *et al.* Lung collagens perpetuate pulmonary fibrosis via CD204 and M2 macrophage activation. *PLoS One* **8**, 1–10 (2013).
 28. Sadtler, K. *et al.* Developing a pro-regenerative biomaterial scaffold microenvironment requires T helper 2 cells. *Science (80-.)*. **352**, 366–370 (2016).
 29. Artym, V. & Matsumoto, K. Imaging Cells in Three-Dimensional Collagen Matrix. *Curr. Protoc. Cell Biol.* 1–23 (2010). doi:10.1002/0471143030.cb1018s48.Imaging
 30. Dobin, A. *et al.* STAR: ultrafast universal RNA-seq aligner. *Bioinformatics* **29**, 15–21 (2013).
 31. Heinz, S. *et al.* Simple combinations of lineage-determining transcription factors prime cis-regulatory elements required for macrophage and B cell identities. *Mol. Cell* **38**, 576–89

- (2010).
32. Taciak, B. *et al.* Evaluation of phenotypic and functional stability of RAW 264.7 cell line through serial passages. *PLoS One* **13**, 1–13 (2018).
 33. Wullkopf, L. *et al.* Cancer cells' ability to mechanically adjust to extracellular matrix stiffness correlates with their invasive potential. *Mol. Biol. Cell* **29**, 2378–2385 (2018).
 34. Balwiercz, P. J. *et al.* ISMARA: automated modeling of genomic signals as a democracy of regulatory motifs. *Genome Res.* **24**, 869–884 (2014).
 35. Dupont, S. *et al.* Role of YAP/TAZ in mechanotransduction. *Nature* **474**, 179–183 (2011).
 36. Viola, A., Sarukhan, A., Bronte, V. & Molon, B. The pros and cons of chemokines in tumor immunology. *Trends in Immunology* **33**, 496–504 (2012).
 37. Griffith, J. W., Sokol, C. L. & Luster, A. D. Chemokines and Chemokine Receptors: Positioning Cells for Host Defense and Immunity. *Annu. Rev. Immunol.* **32**, 659–702 (2014).
 38. Coelho, A. L. *et al.* The Chemokine CCL6 Promotes Innate Immunity via Immune Cell Activation and Recruitment. *J. Immunol.* **179**, 5474–5482 (2007).
 39. Zelenay, S. *et al.* Cyclooxygenase-Dependent Tumor Growth through Evasion of Immunity. *Cell* **162**, 1257–1270 (2015).
 40. Kuczek, D. E. *et al.* Collagen density regulates the activity of tumor-infiltrating T cells. *bioRxiv* (2018). doi:10.1101/493437
 41. Salmon, H. *et al.* Matrix architecture defines the preferential localization and migration of T cells into the stroma of human lung tumors. *J. Clin. Invest.* **122**, 899–910 (2012).
 42. Hartmann, N. *et al.* Prevailing role of contact guidance in intrastromal T-cell trapping in human pancreatic cancer. *Clin. Cancer Res.* **20**, 3422–3433 (2014).

Table 1. Most up- and downregulated genes between macrophages grown in low-density (1 mg/ml) collagen vs. high-density (4 mg/ml) collagen matrices.

Upregulated genes			Downregulated genes		
Gene name	Fold change	FDR	Gene name	Fold change	FDR
<i>Arid5a</i>	2,9254116	4,05705E-46	<i>Cplx2</i>	-2,8868824	7,48E-25
<i>Cish</i>	2,6576232	4,76828E-59	<i>Prss35</i>	-2,3292416	5,27E-126
<i>Anxa3</i>	2,3248294	1,18564E-70	<i>Fam20a</i>	-2,3123299	5,12E-25
<i>Aldh1l2</i>	2,1700798	1,54229E-43	<i>Col27a1</i>	-1,9942138	8,01E-24
<i>Glpr2</i>	2,0847995	3,46E-34	<i>Ndrp4</i>	-1,8407066	4,51E-101
<i>Trem1</i>	1,8953033	3,87453E-44	<i>Serpina6b</i>	-1,8248986	1,89E-45
<i>Siglec1</i>	1,7143361	4,87E-36	<i>Rab15</i>	-1,6311314	2,60E-33
<i>Gm14023</i>	1,6057289	3,51E-34	<i>Fggy</i>	-1,5203824	6,47E-25
<i>Il1a</i>	1,5978122	8,87E-35	<i>Tm4sf19</i>	-1,4549952	3,51E-34
<i>Klhl6</i>	1,5393846	9,71E-40	<i>Stc1</i>	-1,3335709	1,92E-43

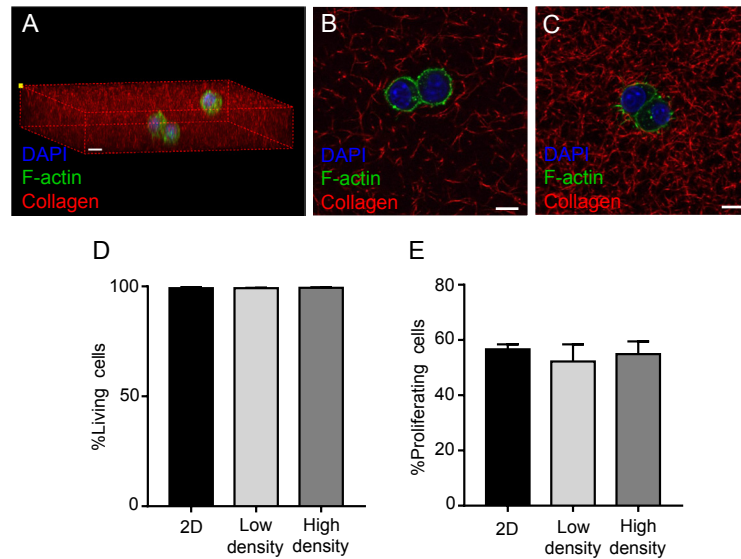


Figure 1. Collagen density does not affect viability and proliferation of RAW 264.7 macrophages. (A-C) Representative confocal microscopy images of RAW 264.7 macrophages grown in 3D collagen matrices of 1 mg/ml (low density, A and B) or 4 mg/ml (high density, C) collagen. (A) 3D projection of collagen embedded RAW 264.7 macrophages. (B and C) Single sections of RAW 264.7 macrophages embedded in collagen. (A-C) Scale bars = 10 μm. (D and E) RAW 264.7 macrophages were cultured for three days in the indicated conditions and analyzed by flow cytometry to assess viability (D) and proliferation (E). The results are based on three individual experiments with three samples per condition in each. Error bars = SEM.

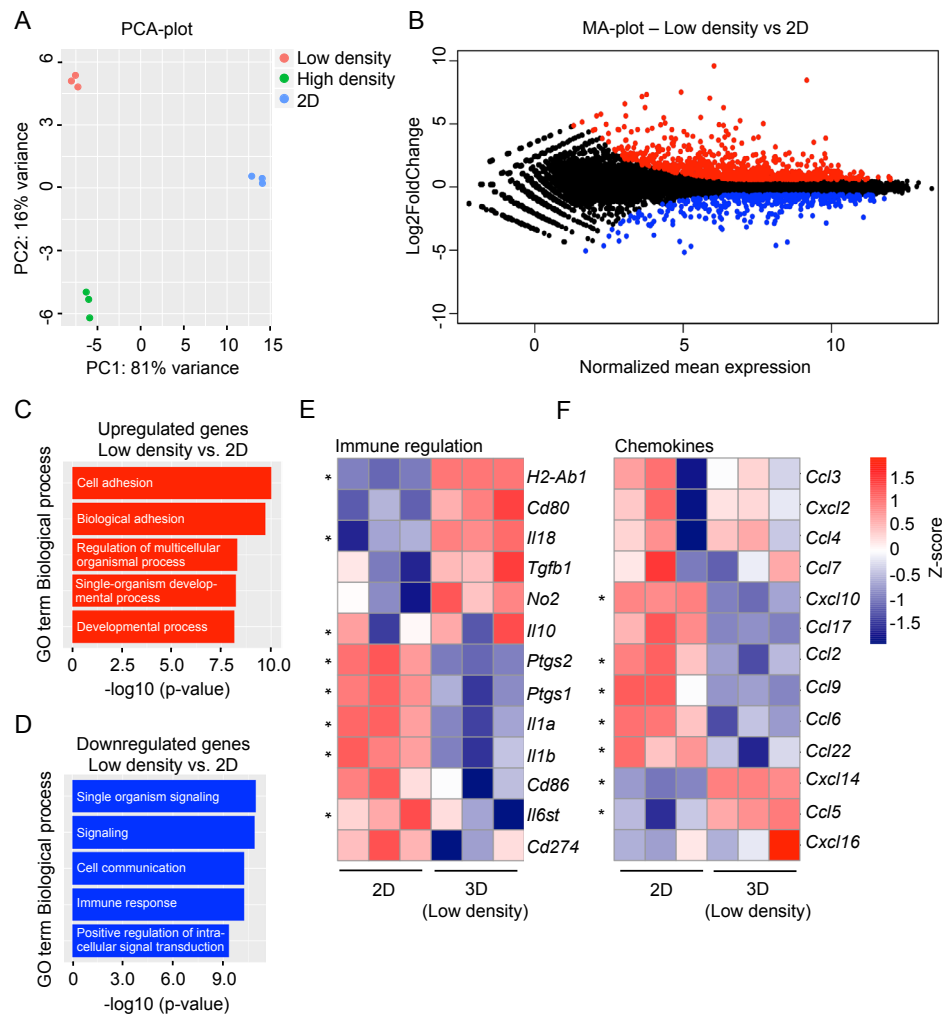


Figure 2. 3D culture changes the gene expression profile of RAW 264.7 macrophages. RNA was extracted from RAW 264.7 macrophages cultured in collagen matrices of 1 mg/ml (Low density) or 4 mg/ml (High density) collagen or on tissue-culture treated plastic (2D) and analyzed using RNA sequencing. (A) Principal component analysis (PCA) plot of RAW 264.7 macrophages cultured in the indicated conditions. (B) MA-plot of differentially expressed genes between RAW 264.7 macrophages grown in 3D in low-density collagen or on tissue-culture treated plates. Red and blue dots illustrate genes that are significantly upregulated and downregulated, respectively, in cells cultured in 3D in low-density collagen compared to 2D cultured cells (FDR < 0.01 and Log2Fold Change ± 0.584962501). (C and D) GOseq analysis of all differentially upregulated genes (C) or downregulated genes (D) between RAW 264.7 cells grown in low-density collagen and on tissue-culture treated plastic. (E and F) Heat maps of the gene expression levels of a panel of selected genes involved in immune regulation (E) or encoding chemokines (F). Z-score = Normalized RPKM values. * = p-value < 0.05.

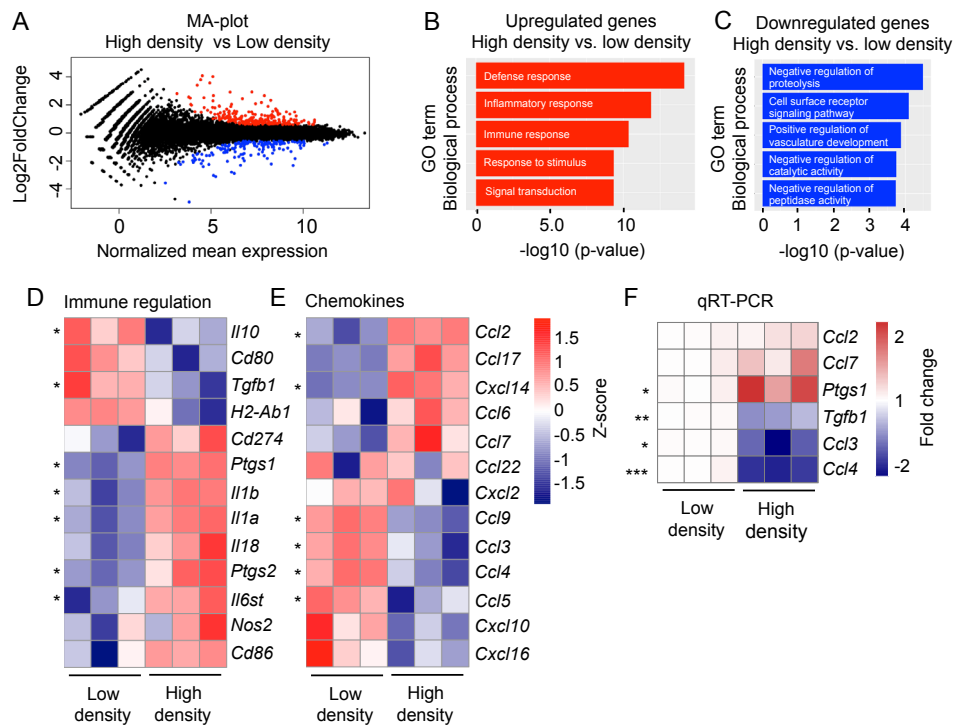


Figure 3. Collagen density regulates genes associated with immune regulation and genes encoding chemokines. RNA was extracted from RAW 264.7 macrophages cultured in collagen matrices of 1 mg/ml (Low density) or 4 mg/ml (High density) collagen and analyzed using RNA sequencing. (A) MA-plot of differentially expressed genes between RAW 264.7 macrophages cultured in low- and high density collagen. Red and blue dots illustrate genes that are significantly upregulated and downregulated, respectively, in cells cultured in 3D in high-density collagen compared to low-density collagen (FDR < 0.01 and Log2Fold Change +/- 0.584962501). (B and C) GOseq analysis of all differentially upregulated (B) and downregulated (C) genes between RAW 264.7 macrophages cultured in low and high density collagen matrices. (D and E) Heat maps of the gene expression levels of a panel of selected genes involved in immune regulation (D) or encoding chemokines (E). Z-score = Normalized RPKM values. * = p-value < 0.05. (F) qRT-PCR analysis of RAW 264.7 macrophages cultured in low and high density collagen. Data were obtained from three individual experiments with four samples of each condition. * = p-value < 0.05. ** = p-value < 0.01. *** = p-value < 0.001.

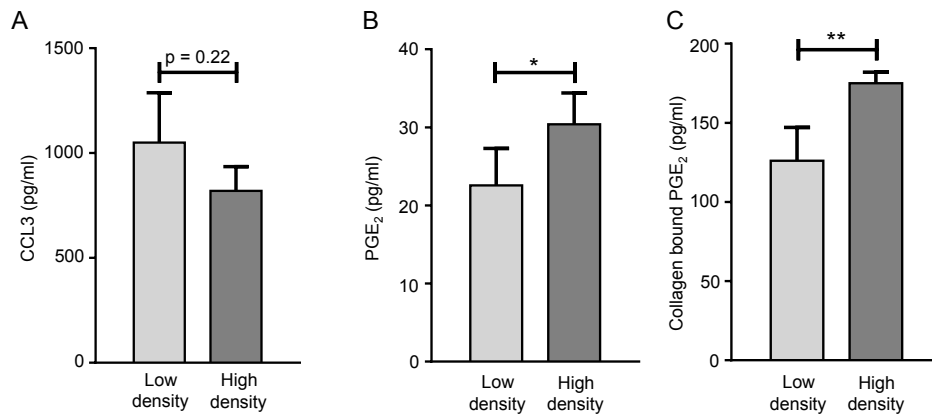


Figure 4. RAW 264.7 macrophages grown in high density collagen secrete less CCL3 and more PGE2. (A) CCL3 ELISA measurements of conditioned media from RAW 264.7 macrophages cultured in collagen matrices of 1 mg/ml (Low density) or 4 mg/ml (High density) collagen. (B) Prostaglandin E2 (PGE₂) ELISA measurements of conditioned media from RAW 264.7 macrophages cultured in collagen matrices of low- or high density. Data are obtained from three (A) or two (B) individual experiments. Error bars = SEM. (C) ELISA measurements of collagen-bound PGE₂ from RAW 264.7 macrophages cultured in collagen matrices of low- or high density. Error bars = SD. * = p-value < 0.05. ** = p-value < 0.01

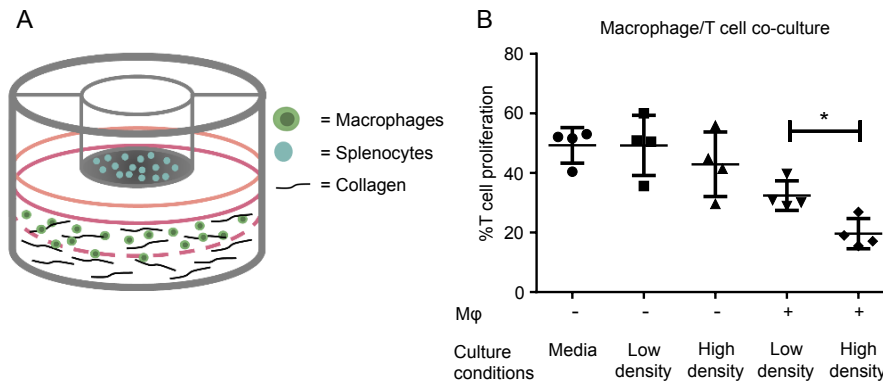


Figure 5. Collagen density regulates T cell proliferation through its effects on RAW 264.7 macrophages. (A) Splenocytes were isolated from the spleens of BALB/c mice. The cells were co-cultured with RAW 264.7 macrophages grown in collagen matrices of 1 mg/ml (low density) or 4 mg/ml (high density). All samples were supplemented with 5 μ g/ml Concanavalin A (ConA). As controls, splenocytes were cultured above collagen matrices of low- or high collagen density without any embedded RAW 264.7 macrophages. After three days of co-culture the proliferation of T cells was measured using a BrdU based flow cytometry assay. Error bars = SD. * = p-value < 0.05.

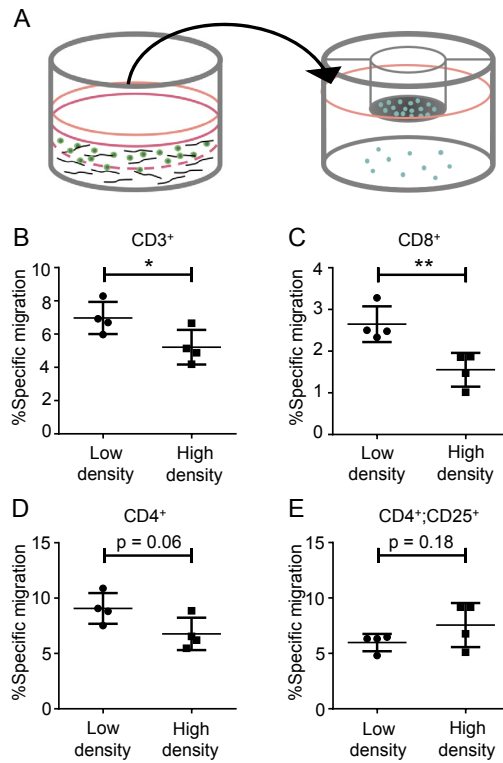


Figure 6. Collagen density alters the chemotactic activity of RAW 264.7 macrophages. (A) Isolated murine T cells were cultured in transwell inserts with 5 μ m pore size above conditioned media from RAW 264.7 macrophages cultured in 1 mg/ml (low density) or 4 mg/ml (high density) collagen matrices. All samples were supplemented with 3 μ g/ml Concanavalin A (ConA). (B-E) After 26-28 hours of culture the migration of T cells was examined by flow cytometry. Error bars = SD. * = p-value < 0.05. ** = p-value < 0.01